304 Letters to the Editor

References

- [1] Witteles RM, Fowler MB. Insulin-resistant cardiomyopathy clinical evidence, mechanisms, and treatment options. | Am Coll Cardiol 2008;51:93–102.
- [2] Hsueh WA, Lyon CJ, Quinines MJ. Insulin resistance and the endothelium. Am J Med 2004:117:109–17.
- [3] Vitale C, Mercuro G, Cornoldi A, Fini M, Volterrani M, Rosano GMC. Metformin improves endothelial function in patients with metabolic syndrome. J Intern Med 2005;258:250–6.
- [4] Andreadis EA, Katsanou PM, Georgiopoulos DX, et al. The effect of metformin on the incidence of type 2 diabetes mellitus and cardiovascular disease risk factors in overweight and obese subjects—the Carmos study. Exp Clin Endocrinol Diabetes 2009: 117:175–80.
- [5] Braun B, Eze P, Stephens BR, et al. Impact of metformin on peak aerobic capacity. Appl Physiol Nutr Metab 2008:33:61–7.
- [6] Nohria A, Gerhard-Herman M, Creager MA, Hurley S, Mitra D, Ganz P. Role of nitric oxide in the regulation of digital pulse volume amplitude in humans. J Appl Physiol 2006;101:545–8.
- [7] Kuvin JT, Patel AR, Sliney KA, et al. Assessment of peripheral vascular endothelial function with finger arterial pulse wave amplitude. Am Heart J 2003;146:168–74.
- [8] Coats AJS, Shewan LG. Statement on Authorship and Publishing Ethics in the International Journal of Cardiology. Int J Cardiol Dec 2 2011;153(3):239–40.

- [9] Wasserman K, Hansen JE, Sue DY, Whipp BJ. Principles of exercise testing and interpretation. Philadelphia: Lippincott Williams & Wilkins; 1987. p. 72–85. Normal values
- [10] Myers J, Prakash M, Froelicher V, Do D, Partington S, Atwood JE. Exercise capacity and mortality among men referred for exercise testing. N Engl J Med 2002;346:793–801.
- [11] Batandier C, Guigas B, Detaille D, et al. The ROS production induced by a reverseelectron flux at respiratory-chain complex 1 is hampered by metformin. J Bioenerg Biomembr 2006;38:33–42.
- [12] El-Mir MY, Nogueira V, Fontaine E, Avéret N, Rigoulet M, Leverve X. Dimethylbiguanide inhibits cell respiration via an indirect effect targeted on the respiratory chain complex I. J Biol Chem 2000;275:223–8.
- [13] Guigas B, Detaille D, Chauvin C, et al. Metformin inhibits mitochondrial permeability transition and cell death: a pharmacological in vitro study. Biochem J 2004:382:877–84.
- [14] Owen MR, Doran E, Halestrap AP. Evidence that metformin exerts its anti-diabetic effects through inhibition of complex 1 of the mitochondrial respiratory chain. Biochem I 2000:348(Pt 3):607–14.
- [15] Leverve XM, Guigas B, Detaille D, et al. Mitochondrial metabolism and type-2 diabetes: a specific target of metformin. Diabetes Metab 2003;29:6S88-6S94.
- [16] Müller MM, Griesmacher A. Markers of endothelial dysfunction. Clin Chem Lab Med 2000;38:77–85.

0167-5273/\$ – see front matter © 2012 Elsevier Ireland Ltd. All rights reserved. doi:10.1016/j.ijcard.2012.04.113

Dynamic assessment of aortic annulus in patients with aortic stenosis throughout cardiac cycle with dual-source computed tomography

Li-qing Peng a, Zhi-gang Yang a,b,*, Jian-qun Yu a, Zhi-gang Chu a, Wen Deng a, Heng Shao a

^a Department of Radiology, West China Hospital, Sichuan University, Chengdu, Sichuan, China

ARTICLE INFO

Article history: Received 19 April 2012 Accepted 22 April 2012 Available online 15 May 2012

Keywords:
Aortic stenosis
Aortic valve
Dual-source computed tomography
Catheter
Cardiac-gated imaging technique

Precise measurement of aortic annular diameter (AAD) is critical for choosing appropriate prosthetic valve size for transcatheter aortic valve implantation (TAVI), because annulus-prosthesis mismatch due to inaccurate sizing of the prosthesis may lead to paravalvular aortic regurgitation [1,2]. Cardiac pulsatility and aortic compliance may result in aortic annulus changes [3]. However, the dynamic changes of aortic annulus during the cardiac cycle have not been clarified in patients with aortic stenosis (AS) [4–6]. Knowledge of the dynamic characteristics of aortic annulus in this population may improve our understanding of aortic annulus and help accurately size aortic annulus. Thus, we aimed to determine the dynamic features of aortic annulus in patients with severe AS throughout cardiac cycle with retrospectively ECG-gated dual-source computed tomography (DSCT) angiography.

E-mail address: yangzg6666@yahoo.com.cn (Z. Yang).

From December 2009 to October 2011, 62 patients (mean age: 68.2 ± 5.9 years, range: 60-82 years; 41males, 21 females) with severe tricuspid AS who underwent retrospective ECG-gated DSCT angiography were included.

All patients were scanned by a DSCT scanner (Somatom Definition, Siemens Medical Solutions, Germany). Scan range was from 2 cm caudal to the level of the tracheal bifurcation to the diaphragm. Scan was performed using retrospectively ECG-gated mode. Full tube current was used throughout R–R interval. The scanning parameters were as follows: collimation, 64×0.6 mm; gantry rotation time, 330 ms; Pitch (heart rate dependent: 0.2–0.5). Body mass index (BMI) dependent tube voltage: 100-120 kV; BMI dependent tube current: 220-330 mAs. All patients received 70-75 ml nonionic contrast media (iopamidol, 370 mg/ml; Bracco Sine Pharmaceutical Corp. Ltd, Shanghai, China) through an antecubital vein with a power injector (Stellant, Medrad, Inianola, USA) at a flow rate of 5.0 ml/s.

Ten data sets of axial images (0%–90%) at 10% step of the R-R interval were reconstructed with a slice thickness of 1 mm and an increment of 1 mm. The data sets were analyzed using cardiac post-processing software (Syngo Circulation, Siemens Medical Solutions).

For evaluating aortic annulus, the major and minor AADs were measured on the plane created at the base of implantation of three aortic cusps (Fig. 1). The dynamic changes of AAD during cardiac cycle were expressed as absolute difference [maximum — minimum of major AAD] or [maximum — minimum of minor AAD] during entire R-R interval for further analysis. To test the agreement of measurements on DSCT and echocardiography, the AAD on three chamber view (similar to parasternal long-axis view on echocardiography) was measured on 20% phase (Fig. 2). To determine the determinants of the dynamic changes of AAD, we measured the variables of calcium score, aortic valve area (AVA), diameters of sinotubular junction (STJ), diameters of left ventricular outflow tract (LVOT) and stroke volume (Figs. 3 and 4). Degree of AS, mean pressure gradient of aortic valve and stroke volume

^b State Key Laboratory of Biotherapy, West China Hospital, Sichuan University, Chengdu, Sichuan, China

^{*} Corresponding author at: Department of Radiology, West China Hospital, Sichuan University, 37# Guo Xue Xiang, Chengdu, Sichuan 610041, China. Tel./fax: +86 28 85423817

Letters to the Editor 305

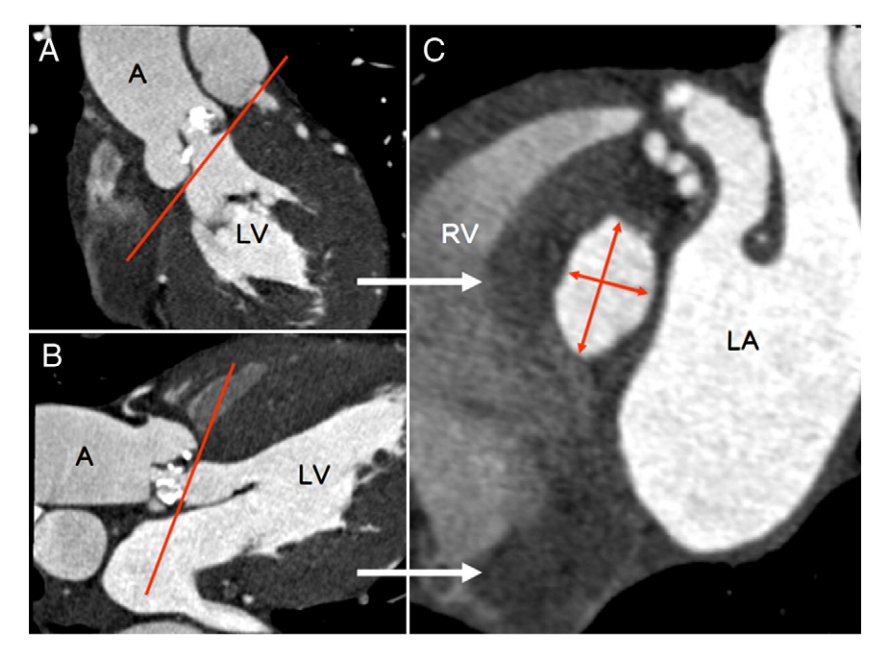


Fig. 1. Measurement of aortic annular diameters.-A, B: Aortic annulus is defined at the base of implantation of three aortic cusps (red line).-C: Measurement of major and minor aortic annular diameters (red arrows).-(LV = left ventricle, RV = right ventricle, LA = left atrium, A = aorta).

were measured on trans-thoracic echocardiography (TTE). The AAD was measured on parasternal long-axis view on TTE. Intra- and inter-observer variabilities for measuring AAD were performed in 20 randomly selected patients.

Intra-observer variabilities of AAD measurements were $3.8\% \pm 2.3\%$ and $3.9\% \pm 2.4\%$ for major and minor AADs, respectively, while inter-observer variabilities of AAD measurements were $3.9\% \pm 2.7\%$ mm and $4.0\% \pm 2.7\%$ mm for the major and minor AADs, respectively.

In patients with tricuspid severe AS, major AADs were statistically larger than minor AADs in all 10 phases (each p < 0.05). Major and minor AADs varied throughout the cardiac cycle. The maximum and minimum of major AADs were 28.2 ± 4.0 mm (22.2–37.6 mm) and 27.1 ± 3.7 mm (18.9–36.4 mm) in 0% and 50% R–R intervals, respectively. The maximum and minimum of minor AADs were 23.1 ± 2.6 mm (18.1–28.8 mm) and 21.1 ± 2.8 mm (15.2–26.0 mm) in 10% and 50% R–R intervals, respectively (Fig. 5). The absolute differences of major and that of minor AADs during cardiac cycle were 3.2 ± 1.4 mm (0.4–7.5 mm) and 3.6 ± 1.4 mm (0.5–8.7 mm), respectively (Table 1). The absolute differences of major and minor AADs that exceeded 3 mm were found in 42 (66.7%) and 44 (71.0%)

of 62 patients, respectively. There was good agreement between DSCT and TTE for AAD measurement (23.1 \pm 2.6 mm vs. 21.4 \pm 2.07 mm), as assessed with Bland-Altman plot analysis (Fig. 6).

To determine the independent determinants of dynamic changes of aortic annular dimension in patients with severe AS, multivariate linear regression analysis was performed, adjusted for age, gender, mean diameter of STJ, mean diameter of LVOT, calcium score, AVA, mean pressure gradient, stroke volume and pulse pressure. Multivariate linear regression analysis showed that mean diameter of LVOT and stroke volume were independently associated with greater absolute differences of major AAD and minor AAD (standardized $\beta = 0.345$, P = 0.034 vs. standardized $\beta = 0.376$, P = 0.02) on DSCT, respectively (Table 2).

In our study, we noted that major AAD was statistically larger than minor AAD in patients with tricuspid severe AS, which indicated aortic annulus as an asymmetrical geometry. Our result was consistent with previous studies [1,4,7]. Moreover, our series showed that AAD varied significantly during cardiac cycle with the absolute difference of AAD over 3 mm in part of the patients with severe AS. For these patients, dynamic changes of aortic annulus might influence the accuracy for



Fig. 2. Measurement of aortic annular diameter on three chamber view (red arrow). (Abbreviations as in Fig. 1).

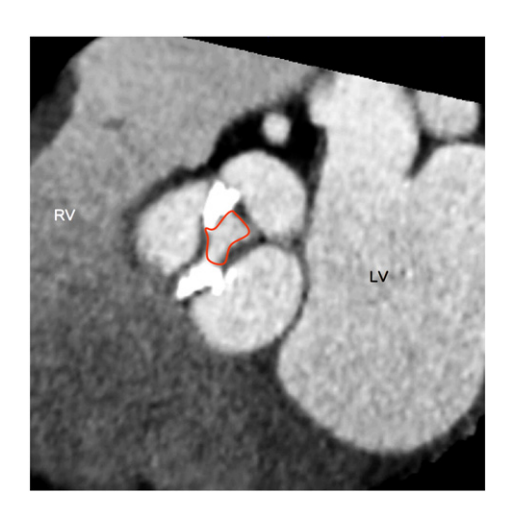


Fig. 3. Planimetry of aortic valve area at short-axis view of aorta (red loop). (Abbreviations as in Fig. 1).

Download English Version:

https://daneshyari.com/en/article/2929953

Download Persian Version:

https://daneshyari.com/article/2929953

<u>Daneshyari.com</u>